Program Digest, 2019 IEEE International Ultrasonics Symposium (IUS)
Glasgow, Scotland, October 6-9, 2019

Single Microbubble Measurements for Bound and Unbound Conditions

Jordan S. Lum
Department of Mechanical Engineering
University of Colorado
Boulder, USA
Jordan.Lum@colorado.edu

Verya Daeichin
Department of Applied Sciences
Delft University of Technology
The Netherlands
V.Daeichin@tudelft.nl

Todd W. Murray
Department of Mechanical Engineering
University of Colorado
Boulder, USA
Todd.Murray@colorado.edu

Mark A. Borden
Department of Mechanical Engineering
University of Colorado
Boulder, USA
Mark.Borden@colorado.edu

We show here that adhesion to a solid substrate increases the resonance frequency of a lipid-coated microbubble by causing an apparent increase in shell stiffness. Using our previously developed photoacoustic measurement technique to drive individual microbubbles into small-amplitude oscillations, we found that biotinylated microbubbles adherent to a streptavidin-coated glass coverslip had much higher resonance frequencies than unbound microbubbles. The frequency responses of the bound microbubbles agree well with a linearized form of the modified Rayleigh-Plesset model with an added increase of shell elasticity. The apparent shell elasticity increased from 0.5 N/m for unbound microbubbles to 2.6 N/m. These findings may be used to better understand microbubble dynamics for applications in ultrasound imaging and therapy.

Keywords—adhesion, shell elasticity, resonance frequency

I. Introduction

Lipid-coated microbubbles are being studied for use in ultrasound imaging and therapy [1], [2]. Although much of the research on the acoustic response of an individual microbubble assumes it is in an isotropic medium, there has been interest in changes in acoustic response and stability for microbubbles that are adhered to a substrate compared to those that are unbound [3]. All of these studies for adherent microbubbles have used acoustic driving pressures significant enough to induce nonlinear responses and decreased stability of the bound microbubbles [4]–[8]. However, there has still been a lack of clear understanding for the physical dynamics that a bound microbubble undergoes during oscillations. Thus, the purpose of this study was to investigate the small-amplitude radial oscillations of individual microbubbles using a sensitive photoacoustic technique we previously developed to better understand the changes in microbubble dynamics when it is bound and not bound to a solid substrate.

II. Materials and Methods

A. Preparation of Lipid-Shelled Microbubble Samples

Fabrication and preparation of microbubble samples for these experiments followed similar procedures from our previous study [9]. Briefly, non-biotinylated control microbubbles were fabricated with phospholipid shells consisting of 1,2-dipalmitoyl-sn-glycero-3-phosophocholine (DPPC) and 1,2-distearoyl-sn-glycerol-3-phosphoethanolamine-N-[methoxy(polyethylene glycol)-2000] (DSPE-PEG2000) at a molar ratio of 90:10. The biotinylated microbubbles were fabricated with a lipid shell composed of DPPC, DSPE-PEG2000, and 1,2-distearoyl-sn-glycerol-3-phosphoethanolamine-N-[biotinyl-(polyethylene glycol)-2000] (DSPE-PEG2000-B) at a molar ratio of 90:9:1. All lipid materials were purchased from Avanti Polar Lipids (Alabaster, AL) and were suspended in 40-mL of phosphate-buffered saline (PBS) at a total lipid concentration of 2 mg/mL. Using a Branson 450 Sonifier (Danbury, CT) set at a low power setting (2/10), the lipid solution was mixed and heated until the suspension appeared translucent and reached above a temperature of 51 °C. A 2-mL aliquot of the lipid suspension was then pipetted into a 3-mL glass serum vial where the headspace was exchanged to contain perfluorobutane (PFB) gas at 99 wt% purity purchased from FluoroMed (Round Rock, TX). A TPC D-650 Amalgamator was used to generate microbubbles by vigorously shaking the serum vial at 4,250 RPM for 40 seconds. To ensure solidification of the lipid shells after microbubble fabrication, the microbubbles were quickly quenched to room temperature in an ice bath. A differential centrifugation technique [10] was used to remove excess residual lipid from the solution and any microbubbles outside of a size range of ~2 to 5 μm in radius.

Sample preparation involved 70 μL of diluted microbubbles (approximately 5×10^5 bubbles per mL) injected between a microscope slide and a streptavidin-modified glass cover slip, separated by a thin 15 mm x 15 mm gasket (Bio-Rad Laboratories, Hercules, CA). The streptavidin-modified glass

cover slips were 50 x 24 mm #1 type purchased from Fisher Scientific (Pittsburgh, PA, USA). They were incubated in a streptavidin-PBS solution at room temperature for 1 hour. The streptavidin-PBS solution contained 33 µg/mL concentration of streptavidin that was purchased from Sigma-Aldrich (St. Louis, MO, USA). After incubation, the glass cover slips were gently rinsed with pure PBS solution to remove any excess streptavidin not bound to the surface, and the glass cover slips were completely air-dried before being used for experiments. All glass surfaces were prepared immediately prior to experiments and all microbubbles were tested within 12 hours of fabrication.

B. Photoacoustic Technique for Single Bubble Measurements

Fig. 1 shows a diagram of the experimental setup. The photoacoustic measurement approach has been described in detail in previous work [9]. Briefly, individual microbubbles were driven into small-amplitude radial oscillations using an intensity-modulated continuous wave laser that had a wavelength of 1550 nm. The output of the laser was sent through a 50x magnification microscope objective where it had a 1/e diameter of 3 µm and an optical power of 5.5 mW at the focal plane of the sample. The fluid was illuminated approximately 100 µm away from the microbubble of interest. The excitation laser was absorbed by the water to generate ultrasonic waves through the photoacoustic effect, thus driving the microbubble into oscillation. A second continuous wave laser with a wavelength of 532 nm was used to detect the small-amplitude oscillations of the microbubble through forward light scattering. This detection laser was passed through the same microscope objective and had a 1/e diameter of 9.5 µm and an optical power of 1.0 mW at the focal plane of the sample where it illuminated the single microbubble. The forward light scatter from the microbubble was then recorded using a photodetector and a radio frequency lock-in amplifier. The frequency of the intensity-modulation for the excitation laser source was swept across a range of at least 2 MHz in 50 kHz steps to generate a resonance curve for the microbubble of interest. Images of the microbubbles were recorded using a CCD camera, and these were subsequently used to determine the resting radius.

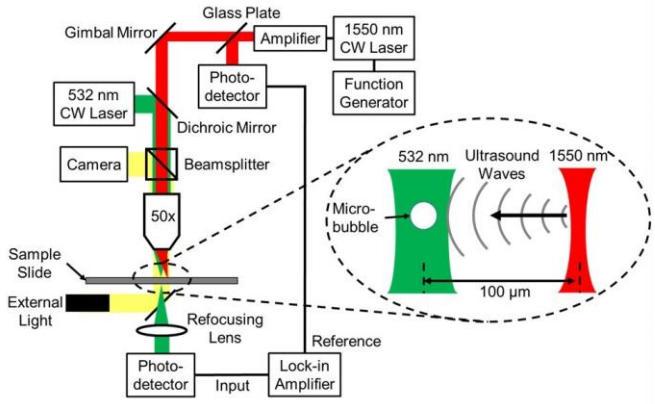

Fig. 1 A diagram of the photoacoustic experimental setup used to excite and measure small-amplitude oscillations of single microbubbles.

C. Analysis of Microbubble Dynamic Response

Fig. 2 shows example resonance curves for a biotinylated and non-biotinylated microbubble, both with a radius of 2.7 µm. The experimental data for each bubble were best fit with a Lorentzian curve. Here, the resonance frequency, *f*, of the microbubble was defined as the frequency at the maximum amplitude, and the damping ratio, ζ, was defined as, $\zeta=\Delta f/2f$, where Δf was the full width at the half-maximum of the resonance curve.

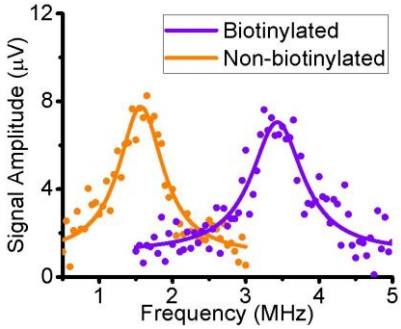

Fig. 2 Resonance curves for single biotinylated and non-biotinylated microbubbles with radii of 2.7-µm. Data were best fit with the Lorentzian curves shown by the solid curves.

A linearized form of the modified Rayleigh-Plesset model from Sarkar *et al*. [11] for small-amplitude oscillations was used to calculate the microbubble lipid shell elasticity, χ. The expression for lipid shell elasticity is given as:

$$\chi = 1.44\pi^2 f^2 \rho_L {R_0}^3/(1-2\zeta^2) - 3\kappa P_0 R_0/4 - \sigma(R_0)(3\kappa-1)/2 \quad (1)$$

where ρ_L is the density of the surrounding fluid (10^3 kg/m^3), R_0 is the resting radius of the microbubble, κ is the polytropic exponent for the gas core, P_0 is the ambient pressure (10^5 Pa), and $\sigma(R_0)$ is the surface tension of the gas-liquid interface (assumed to be negligible). The polytropic exponent was calculated assuming an air gas core which resulted in a range of values from 1.04 to 1.10 [12], [13]. Equation (1) also compensates for the expected 17% eigenfrequency decrease due to the microbubbles oscillating next to the glass coverslip which acts as a rigid boundary [14].

III. Results and Discussion

Bound versus Non-bound Microbubble Responses

Fig. 3 is a plot of eigenfrequency as a function of bubble radius for the measurements of 52 biotinylated microbubbles and 53 non-biotinylated control microbubbles. The median lipid shell elasticity calculated for the targeted microbubbles was χ=2.6 N/m, and the non-targeted microbubbles had a median shell elasticity of χ=0.5 N/m. These shell elasticity values were used with Equation 1 to calculate the values shown by the solid curves in Fig. 3. The dashed curve also shown in Fig. 3 represents the response from an unshelled microbubble with χ=0 N/m. From Figs. 2 and 3, the biotinylated microbubbles that were adhered to the solid substrate had much higher resonance frequencies than the control microbubbles that were unbound. There is a slight spread in the frequency response of the biotinylated microbubbles, possibly owing to the heterogeneity of the streptavidin-coated glass surface preventing full contact between the microbubble and the surface.

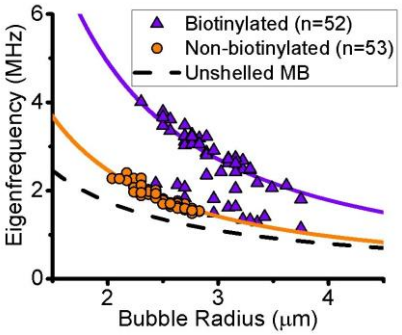

Fig. 3 Eigenfrequency as a function of bubble radius. Measurements from n=52 biotinylated microbubbles are shown by the triangles while the circles represent the 53 non-biotinylated control microbubbles. Solid curves represent the modeled responses from Equation 1 using the median shell elasticity values for each group. The dashed curve represents the response for an unshelled microbubble where shell elasticity is 0 N/m.

IV. Conclusions

In this study, we investigated the small-amplitude radial oscillations of biotinylated microbubbles that were adhered to a streptavidin-coated glass surface. Using a photoacoustic technique that we previously developed, we found adherent microbubbles had higher resonance frequencies than non-bound microbubbles. We attribute this increase in resonance frequency for adherent microbubbles to an additional stiffening effect due to adhesion. These results may help to provide a better understanding of microbubble use in ultrasound imaging and therapy.

Acknowledgment

Funding was provided by NIH grant R01 CA195051 to M.A.B. and a University of Colorado Boulder Mechanical Engineering Research Innovation Fellowship to J.S.L.

References

[1] W. K. Chong, V. Papadopoulou, and P. A. Dayton, "Imaging with ultrasound contrast agents: current status and future," *Abdom. Radiol.*, vol. 43, no. 4, pp. 762–772, Apr. 2018.

[2] S. Wang, J. A. Hossack, and A. L. Klibanov, "Targeting of microbubbles: contrast agents for ultrasound molecular imaging," *J. Drug Target.*, vol. 26, no. 5–6, pp. 420–434, May 2018.

[3] T. van Rooij, V. Daeichin, I. Skachkov, N. de Jong, and K. Kooiman, "Targeted ultrasound contrast agents for ultrasound molecular imaging and therapy," *Int. J. Hyperthermia*, vol. 31, no. 2, pp. 90–106, Feb. 2015.

[4] T. van Rooij, I. Beekers, K. R. Lattwein, A. F. W. van der Steen, N. de Jong, and K. Kooiman, "Vibrational Responses of Bound and Nonbound Targeted Lipid-Coated Single Microbubbles," *IEEE Trans. Ultrason. Ferroelectr. Freq. Control*, vol. 64, no. 5, pp. 785–797, May 2017.

[5] M. Overvelde, V. Garbin, B. Dollet, N. de Jong, D. Lohse, and M. Versluis, "Dynamics of Coated Microbubbles Adherent to a Wall," *Ultrasound Med. Biol.*, vol. 37, no. 9, pp. 1500–1508, Sep. 2011.

[6] S. Zhao, K. W. Ferrara, and P. A. Dayton, "Asymmetric oscillation of adherent targeted ultrasound contrast agents," *Appl. Phys. Lett.*, vol. 87, no. 13, p. 134103, Sep. 2005.

[7] B. L. Helfield, E. Cherin, F. S. Foster, and D. E. Goertz, "The Effect of Binding on the Subharmonic Emissions from Individual Lipid-Encapsulated Microbubbles at Transmit Frequencies of 11 and 25 MHz," *Ultrasound Med. Biol.*, vol. 39, no. 2, pp. 345–359, Feb. 2013.

[8] J. Casey, C. Sennoga, H. Mulvana, J. V. Hajnal, M.-X. Tang, and R. J. Eckersley, "Single Bubble Acoustic Characterization and Stability Measurement of Adherent Microbubbles," *Ultrasound Med. Biol.*, vol. 39, no. 5, pp. 903–914, May 2013.

[9] J. S. Lum, D. M. Stobbe, M. A. Borden, and T. W. Murray, "Photoacoustic technique to measure temperature effects on microbubble viscoelastic properties," *Appl. Phys. Lett.*, vol. 112, no. 11, p. 111905, Mar. 2018.

[10] J. A. Feshitan, C. C. Chen, J. J. Kwan, and M. A. Borden, "Microbubble size isolation by differential centrifugation," *J. Colloid Interface Sci.*, vol. 329, no. 2, pp. 316–324, Jan. 2009.

[11] K. Sarkar, W. T. Shi, D. Chatterjee, and F. Forsberg, "Characterization of ultrasound contrast microbubbles using in vitro experiments and viscous and viscoelastic interface models for encapsulation," *J. Acoust. Soc. Am.*, vol. 118, no. 1, pp. 539–550, Jun. 2005.

[12] K. Sarkar, A. Katiyar, and P. Jain, "Growth and Dissolution of an Encapsulated Contrast Microbubble: Effects of Encapsulation Permeability," *Ultrasound Med. Biol.*, vol. 35, no. 8, pp. 1385–1396, Aug. 2009.

[13] L. Hoff, *Acoustic Characterization of Contrast Agents for Medical Ultrasound Imaging*. Dordrecht: Kluwer Academic, 2001.

[14] M. Strasberg, "The Pulsation Frequency of Nonspherical Gas Bubbles in Liquids," *J. Acoust. Soc. Am.*, vol. 25, no. 3, pp. 536–537, May 1953.